Engineering Research Journal

journal homepage: https://erj.journals.ekb.eg/

Development and Optimization of a Cost-Effective Lightweight Humanoid Robotic Arm for Assistive Applications

Mustafa Mahmoud [1], Mohamed Selmy [2], and Mahmoud Elsamanty [1,3]

[1]Mechanical Engineering Department, Faculty of Engineering at Shoubra, Banha University, Cairo 13518, Egypt

[2]Electrical Engineering Department, Faculty of Engineering at Shoubra, Banha University, Cairo 13518, Egypt

[3]Mechatronics and Robotics Department, School of Innovative Design Engineering, Egypt-Japan University of Science and Technology, Alexandria, Egypt

*Corresponding Author E-mail: mustafa.mahmoud@feng.bu.edu.eg

Abstract

This paper presents the development of a cost-effective, lightweight humanoid robotic arm designed to assist the elderly and vulnerable populations. The study aims to provide specialized robotic arms by utilizing a motion planning method based on human arm biomechanics. The arm, created using 3D printing technology with 40% infill, achieves a weight reduction of over 60%. Low-torque servos and a human-like adaptable gripper further enhance cost efficiency and functionality. The arm features simplified joints and is driven by six modified R/C servomotors with analog feedback for precise angle measurement. System identification shows high accuracy, with joint fit percentages ranging from 87.5% to 97.07%. A PID controller, optimized via genetic algorithm (GA), particle swarm optimization (PSO), and honey badger algorithm (HBA), ensures rapid and accurate positioning. The Simscape library models the arm dynamic behavior, addressing forward and inverse kinematics, workspace, and path planning. These innovations promise to advance assistive technologies significantly.

Keywords: Robotics Arm, Assistive Devices, Humanoid Robotic, 3D Printing, Motion Planning, System Identification, and PID control.

DOI: 10.21608/erj.2024.304971.1076
Received 17 July 2024; Received in revised form 29 July 2024; Accepted 03 August 2024
Available online 01 September 2024

1. Introduction

The human hand is crucial for civilization development. As humans evolved to walk upright, their hands developed functions for balance, interaction, and communication. Studying arm motion helps those who have lost their arms regain daily function and societal value [1]. Humanoid robots, like the model proposed in this paper, mimic the human body. They can walk, manipulate objects, and sometimes imitate facial features. These robots replicate human tasks and may collaborate with people for a better future. Researchers analyze human anatomy to create these robots, which are also used for personal assistance and tasks involving human-designed tools and vehicles [2]. Humanoid robots are valuable for dangerous or remote space exploration, especially with artificial intelligence. Some models, like the one in this paper, focus solely on the upper limb[3].

In recent years, engineers and scientists have developed exoskeleton robots to enhance human muscle strength[4]. These powered, wearable robots use hydraulic or electric actuators to support heavy object transportation, reducing physical fatigue and muscle-skeletal illnesses in operators [1], [5]. Most humanoid arm components in this research are 3D printed using polylactic acid (PLA) to ensure durability, with some parts made of wood to reduce costs[3], [5], [6]. The motion of the proposed six degrees of freedom arm is also investigated and optimized.

The development of humanoid robotic arms has been an area of significant research, focusing on enhancing functionality, cost-efficiency, and adaptability for various applications, particularly assistive technologies. This literature review highlights key advancements and methodologies employed in the field.

Recent studies have emphasized the importance of using lightweight materials and advanced manufacturing techniques to create cost-effective robotic arms. For instance, [7] explored the use of 3D printing technology to reduce the weight and cost of robotic components. The study demonstrated that a 40% infill design could significantly reduce the weight of the arm while maintaining structural integrity. Similarly, investigated the benefits of using composite materials in robotic arm construction, highlighting improvements in strength-to-weight ratios and overall performance.

The implementation of control systems is crucial for the precise operation of robotic arms. PID controllers are commonly used due to their simplicity and effectiveness in various applications. However, traditional methods for tuning PID gains, such as Ziegler-Nichols, often do not yield optimal results. Advanced optimization techniques like genetic algorithms (GA), particle swarm optimization (PSO), and honey badger algorithm (HBA) have been employed to enhance controller performance.[8], [9] provided a comprehensive comparison of these optimization methods, demonstrating their effectiveness in reducing settling time, overshoot, and steady-state error in robotic systems. Further validated these findings through experimental trials, confirming the improved dynamic characteristics of the optimized controllers.

Accurate kinematic modeling is essential for the development of robotic arms, allowing for precise control and movement. The Denavit-Hartenberg (DH) convention is widely used for this purpose, as it simplifies the mathematical modeling of robotic joints and links.[10] utilized the DH convention to model a humanoid robotic arm, demonstrating the importance of forward and inverse kinematics in predicting and controlling the arm's movements. Additionally, employed simulation software to validate the kinematic models, ensuring that the theoretical designs corresponded to real-world performance.

Humanoid robotic arms have significant potential in assistive applications, particularly for the elderly and individuals with physical disabilities. [11] discussed various use cases for robotic arms in home environments, such as assisting with daily tasks like eating, dressing, and personal hygiene. The study emphasized the importance of creating user-friendly and adaptable robotic systems to improve the quality of life for users. [12] explored the role of robotic arms in rehabilitation, providing support during physical therapy exercises and aiding in the recovery process. The adaptability and precise control of these arms make them suitable for tasks requiring delicate or repetitive movements, further highlighting their versatility in assistive technologies.

This paper aims to develop a controller that requires the acquisition of a trajectory for human arm motion. To achieve these purposes, the following procedure followed: the mechanical design for the proposed arm is described in section (2), and the Simscape modeling for the proposed arm and forward, inverse kinematics, and trajectory planning were studied in section (3). Section (4) illustrates the experimental work, including the motors model identification of the optimized PID parameters using Genetic, particle swarm algorithms, and honey badger algorithm (HBA) for different trajectories.

2. Mechanical design of the humanoid arm

After analyzing the motion of a human arm, it was determined to correspond to Z-axis rotation at the shoulder (3 degrees of freedom), elbow (1 degree of freedom), forearm (1 degree of freedom), and wrist (2 degrees of freedom). The proposed robotic arm in this study features six degrees of freedom: shoulder flexion/extension, shoulder adduction/abduction, elbow flexion/extension, elbow supination/pronation, wrist flexion/extension, and ulnar/radial deviation. These joints collectively determine the position and orientation of the humanoid arm's end effector, which is represented by a hand and five fingers[13].

The CAD model of the developed humanoid arm is shown in Fig. 1. The design meticulously integrates mechanisms for the shoulder, elbow, wrist, and gripper to replicate human anatomy while emphasizing durability, efficiency, and flexibility. Using lightweight yet robust materials, as depicted in Fig. 1 (Shoulder Flexion/Extension and Shoulder Adduction/Abduction), the arm balances strength and weight for optimal performance. Each joint is strategically designed with specific degrees of freedom to mimic natural human movements while maintaining simplicity and functionality.

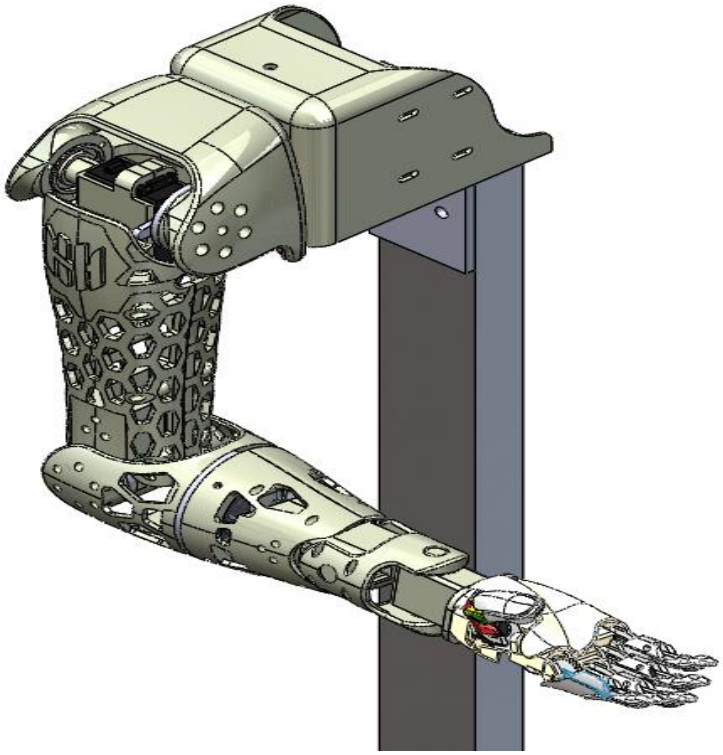

Fig. 1 CAD model of the humanoid arm connected to chest.

The elbow mechanism, shown in Fig. 1 (Elbow Flexion/Extension and Elbow Supination/Pronation), replicates human anatomy with a natural range of motion driven by high-torque servomotors for precise actuation. Similarly, the wrist mechanism, illustrated in Fig. 1 (Wrist Flexion/Extension and Ulnar/Radial Deviation), incorporates multiple degrees of freedom for complex motions, actuated by high-torque servomotors and equipped with sensors for real-time feedback[14], enhancing environmental interaction. Modular components facilitate maintenance and contribute to the humanoid aesthetic.

Table 1 Upper Limb Joint Parameters.

Joint No.	Joints	Min. Required Torque (Kgf.cm)	Motor Torque (Kgf.cm)
1	Shoulder flexion/extension	77.65	100
2	Shoulder adduction/abduction	77.65	100
3	Elbow flexion/extension	32.15	74
4	elbow supination/pronation	6.5	36
5	wrist flexion/extension	6.525	16
6	Ulnar/radial deviation	4.44	16

3. Humanoid Hand Mechanism

The developed hand mechanism closely resembles a human hand, making it adaptable for holding various shapes. It consists of five fingers, designed to operate efficiently with just three servomotors, as illustrated in Fig. 2. The index, middle, and ring fingers are controlled by a single servomotor. At the same time, the pinkie and thumb each have their dedicated servo motors[15]. To achieve this functionality, a series of linkages and gears were incorporated to distribute the motion from the servomotors to the fingers. The central servomotor, responsible for the index, middle, and ring fingers, employs a complex linkage system that ensures coordinated movement, mimicking the natural grasping motion of a human hand. This design not only reduces the number of servomotors required but also minimizes the overall weight and complexity of the hand mechanism.

Each finger is equipped with joints that replicate the human finger range of motion, providing flexibility and dexterity. The thumb, controlled by its servomotor, is positioned and oriented to allow opposition to the other fingers, a crucial feature for grasping and manipulating objects of various shapes and sizes. The pinkie finger, also independently controlled, enhances the hand mechanism's ability to secure and stabilize objects, particularly when dealing with irregular shapes. The servomotors are equipped with feedback mechanisms to provide real-time position and force data[16], enabling precise control and adjustment during operation. This feedback is crucial for tasks requiring delicate handling or when interacting with fragile objects. Additionally, the use of high-torque servomotors ensures that the hand mechanism can exert sufficient force to hold and manipulate heavier objects without compromising stability or control.

Overall, the design of the hand mechanism prioritizes adaptability, efficiency, and reliability, making it a versatile tool for various applications in robotic assistance and rehabilitation. This innovative approach not only enhances the functionality of the humanoid robotic arm but also sets a new benchmark for hand mechanism design in robotic systems.

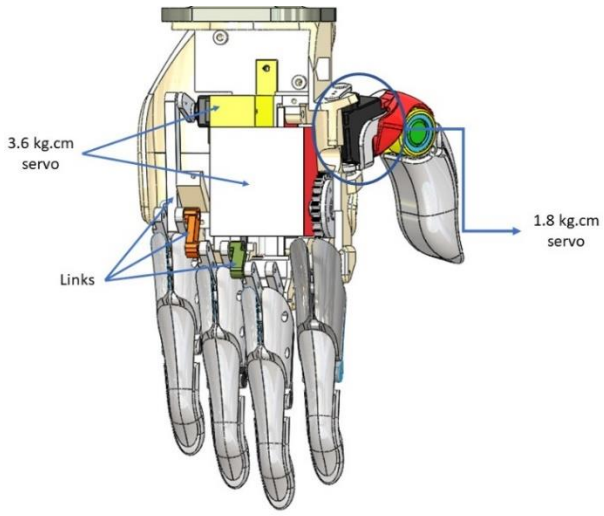

Fig. 2 Humanoid hand cad model

4. Arm Kinematics

4.1 Forward Kinematics

Forward kinematics are instrumental in determining the final position and orientation of the model. This process involves calculating the position and direction of the end-effector based on the given joint parameters. For accurate determination, frame representation is paramount [10]. In this study, the arm kinematic model adheres to the Denavit-Hartenberg (DH) convention, which systematically assigns frames to each joint and link. This convention simplifies the mathematical modeling of the robotic arm movements, ensuring precise calculations of the end-effector's position and orientation. The DH parameters, which include link lengths, twist angles, and offsets, are used to construct the transformation matrices for each joint.

Fig. 3 illustrates the kinematic model of the arm, along with the frames assigned according to the DH convention. Each joint's frame is represented in a manner that facilitates the computation of forward kinematics. The frames provide a reference for the position and orientation of each segment of the arm, enabling a clear and consistent approach to modelling the arm's movements. The implementation of forward kinematics in this research involves a series of transformations that are applied sequentially from the base of the arm to the end-effector. By multiplying the transformation matrices derived from the DH parameters, the overall transformation matrix is obtained. This matrix encapsulates the position and orientation of the end-effector in the Cartesian coordinate system.

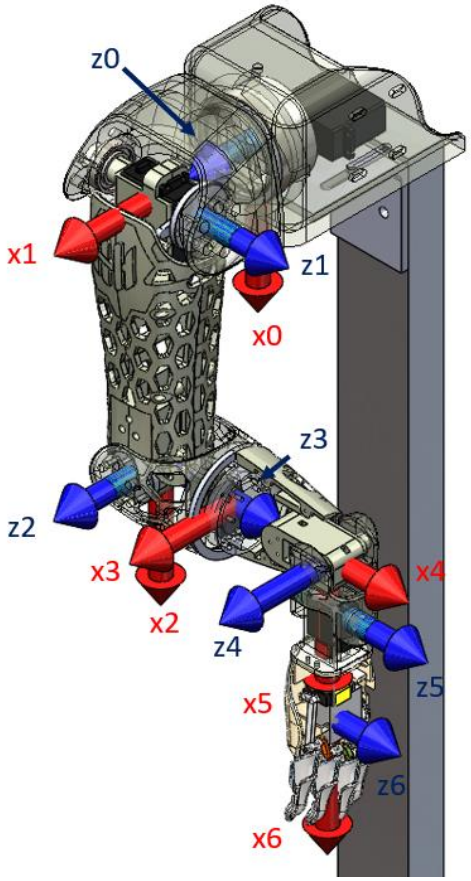

Fig. 3 The arm's joints and frames

Table 2 shows the DH parameters calculated from the humanoid arm robot.

joint	θ	d	a	α
J1	θ_{e1}	90	0	-90
J2	θ_{e2}	0	260	90
J3	θ_{e3}	0	0	-90
J4	θ_{e4}	194.5	0	90
J5	θ_{e5}	0	50	-90
J6	θ_{e6}	0	110	0

4.2 Humanoid Arm joints range and Workspace

By incorporating the motion characteristics of the human arm into the robotic arm, the humanoid motion of the robotic arm can be realized. This process involves mapping the relationships between the human arm's movements and those of the robotic arm. The human arm is composed of three major complex joints: the shoulder complex, the elbow complex, and the wrist joint, as depicted in Fig. 4[17].

In developing the robotic arm, a thorough comparison between the human arm and the robotic arm was conducted. The range of motion for each joint in the robotic arm was designed to match that of the human arm closely. The proposed arm motion ranges for each joint are shown in Table 3, which details the minimum and maximum angle ranges of the humanoid arm[18], [19]. This comparison ensures that the robotic arm can mimic the natural movements of a human arm, enhancing its functionality and adaptability.

Integrating these motion characteristics allows the robotic arm to perform tasks with a level of dexterity and precision similar to that of a human arm. By studying the biomechanics of the human arm, specific ranges of motion were defined for the robotic arm's shoulder, elbow, and wrist joints. This meticulous design ensures that the robotic arm can achieve the necessary movements for various applications, from simple grasping to complex manipulations.

The workspace of the humanoid arm was examined and debated to determine the manipulator robot's restricted mobility range[20]. As shown in **Error! Reference source not found.** (a), the 3 D workspace with a side slice at Y=-59.5mm to extract the 2D workspace for the robot in side-view (X-Z plane) as shown in **Error! Reference source not found.** (b).

Fig. 4 Humanoid arm joints and links

Table 3 Range of active joints of the proposed arm

link		**Theta(rad)**	
No.	**Theta no.**	**min**	**max**
1	Θ1	$-\pi / 2$	$\pi / 2$
2	Θ2	$-\pi / 2$	0
3	Θ3	$-\pi / 2$	0
4	Θ4	$-\pi / 2$	$\pi / 2$
5	Θ5	0	π
6	Θ6	$-\pi / 2$	$\pi / 2$

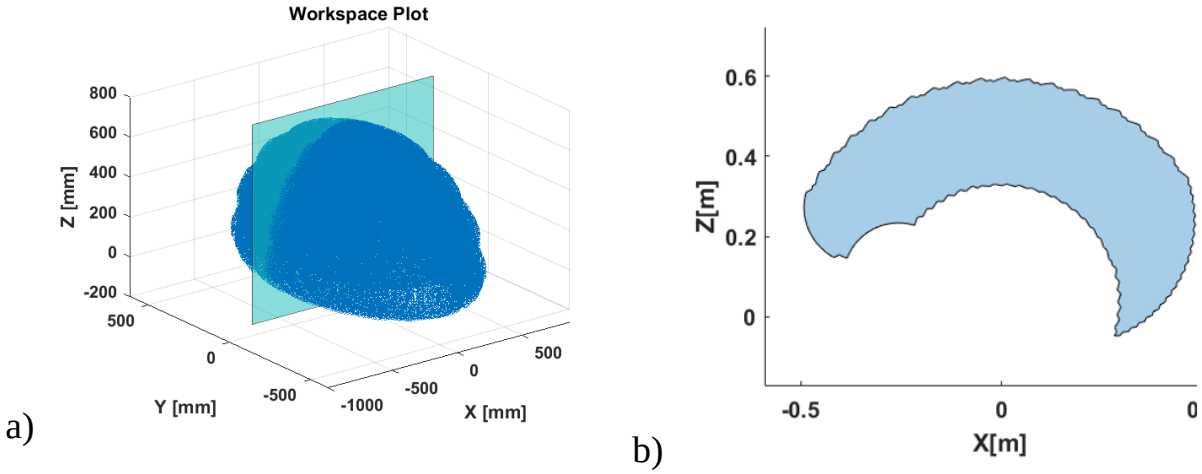

a) b)

Fig. 5 (a)Humanoid arm 3D workspace with slice plane at Y=-59.5 (b) Humanoid arm 2D workspace slice at Y=-59.5

5. Experimental work

The experimental setup involved several key components and steps to ensure accurate control and measurement of the robotic arm's movements as shown in fig.6. Initially, each servomotor was connected to a PWM pin on the Arduino board. The motor's power supply (Vcc) and ground connections were secured to the 5-volt and ground terminals on the Arduino, respectively, ensuring a stable power supply. For accurate joint angle measurement, rotary potentiometers were coupled with each joint of the robotic arm. These potentiometers provided real-time feedback on the joint positions. The potentiometers' outputs were connected to the analog input pins on the Arduino board. This connection allowed the Arduino to read the analog voltage signals corresponding to the joint angles.

Fig. 6 the Experimental setup for the proposed arm

The analog signals from the potentiometers were then processed and converted into precise angle measurements using MATLAB software. The Arduino transmitted these analog signals to the computer, where MATLAB executed the necessary computations to translate the voltage levels into angular positions. This conversion process was essential for real-time monitoring and control of the robotic arm. The Arduino board acted as the central interface, facilitating communication between the servomotors, potentiometers, and the computer. This setup enabled precise control of the servomotors based on the feedback received from the potentiometers[21]. Each servomotor's position could be adjusted accurately to achieve the desired joint angles, ensuring the robotic arm's movements closely mimicked those of a human arm.

Additionally, a custom control algorithm was implemented in MATLAB to manage the PID control of the servomotors. The PID parameters were optimized using advanced techniques such as genetic algorithm (GA), particle swarm optimization (PSO), and honey badger algorithm (HBA) to enhance the system's responsiveness and accuracy. This optimization ensured that the servomotors could achieve rapid and precise positioning, essential for tasks requiring high dexterity and control. The entire system was thoroughly tested to validate its performance. The feedback from the potentiometers was continuously monitored, and the control signals to the servomotors were adjusted in real time to maintain the desired joint angles. This closed-loop control system ensured that the robotic arm operated with high precision and stability, replicating human-like movements effectively.

5.1 System identification

The transfer function for each joint was obtained by using the MATLAB system identification toolbox, inserting the reference signal and the measured one as arrays, and inserting the sampling rate (Ts)[22].

$$Y(s) = \frac{\text{num}(s)}{\text{den}(s)} U(s) + E(s) \quad (1)$$

In this experimental setup, Y(s) represents the model output, which is the system's observed response. The input to the model is denoted as U(s), which is the control signal, or the desired input applied to the system. The difference between the desired input and the observed output is represented by E(s), which is the error signal. This error is crucial for adjusting the control parameters to achieve the desired performance.

Table 4 The obtained transfer functions for the motors moving the six joints.

Joint	equation	Fitness%
Joint 1	$\frac{5708}{s^2 + 465.6s + 5709}$	**95.6%**
Joint 2	$\frac{68.17}{s^2 + 9.345s + 67.87}$	**87.5%**
Joint 3	$\frac{194.6}{s^2 + 20.52s + 194.3}$	**93.97%**
Joint 4	$\frac{194.6}{s^2 + 20.52s + 194.3}$	**97.07%**
Joint 5	$\frac{3218}{s^2 + 44.58s + 3216}$	**96.69%**
Joint 6	$\frac{3218}{s^2 + 44.58s + 3216}$	**90.34%**

5.2 PID controller

The controller plays a crucial role in system control, ensuring that the output aligns with the reference values. PID controllers, illustrated in Fig. 6, are widely used in process industries due to their ability to enhance system response by reducing settling time, overshoot, and steady-state error. Traditional methods for tuning the PID gains, such as Ziegler-Nichols and Chien-Hrones-Reswick, are commonly used but may not always provide optimal results. To achieve superior performance, intelligent computation methods like Genetic Algorithm (GA)[23] and Particle Swarm Optimization (PSO) [24] can be employed for more efficient optimization of the PID parameters. These advanced techniques offer improved accuracy and responsiveness compared to traditional tuning methods. The transfer function of the PID controller can be represented as follows:

$$G_{PID}(s) = K_p + \frac{K_i}{s} + K_d s$$

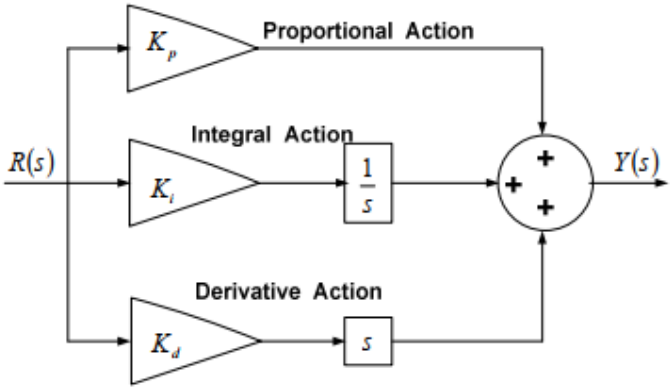

Fig. 7 Block Diagram of PID controller

Where K_p, K_i, and K_d are the proportional, integral, and derivative gains, respectively. Algorithm iterations are performed to determine the optimal PID parameters using the genetic algorithm, particle swarm optimization, and the honey badger algorithm [25].

Table 5 Particle swarm optimization parameters

Parameter	Type/value
No. of iterations	100
No. of particles	50
w	0.9
C_1	2
C_2	2
Fit fun.	Integral time absolute error

Where:

W is the inertia coefficient, C_1 is the personal Acceleration coefficient, and C_2 is the social Acceleration coefficient.

Table 6 Genetic algorithm parameters

Parameter	Type/value
Generation	100
Population size	50
selection	Tournament
Mutation	Adaptive feasible
Crossover	Arithmetic
Fit fun.	Integral time-absolute of error

Table 7 Hony Badger Algorithm parameters

Parameter	Type/value
Honey Badger number	100
β (the ability of a honey badger to get food)	6
C	2
Fit fun.	Integral time-absolute of error

Table 8 PID parameters for each joint are obtained using two optimization techniques: the genetic algorithm, particle swarm optimization, and the honey badge algorithm.

Joint	Algorithm	K_p	K_i	K_d
Joint 1	GA	1	65.80488	0
	PSO	1	65.89404	0
	HBA	1	65.70559	0
Joint2	GA	0.999888	7.58499	0.068931
	PSO	1	7.586916	0.069289
	HBA	1	7.073787	0
Joint3	GA	0.999998	12.57586	0.010777
	PSO	1	12.58496	0
	HBA	1	12.58481	0
Joint4	GA	0.999985	30.762	0.009445
	PSO	1	20.80664	0
	HBA	1	20.86168	0
Joint5	GA	0.939508	47.68741	0.014258
	PSO	1	39.01049	0
	HBA	0.999927	55.36272	0.016789
Joint6	GA	0.999962	64.70607	0.170795
	PSO	1	14.28109	0
	HBA	1	14.2806	0

6. Validation of Kinematic Controller

To validate the kinematic equations of the robotic arm, a comprehensive analysis of a three-dimensional path was conducted. The arm model was initially constructed in SolidWorks, a powerful CAD software, to ensure precise mechanical design and accurate representation of the arm's components and joints. This detailed model was then imported into MATLAB using the SIMSCAPE library, which provides a versatile environment for simulating and analyzing mechanical systems. In the analysis, a specific three-dimensional path, in this case, a square trajectory, was chosen to evaluate the performance and accuracy of the kinematic model. Fig. 7(a) illustrates the square path that the robotic arm is required to follow. The study aimed to compare the desired path with the actual path achieved by the robotic arm, focusing on the first three joints[26].

The robotic arm was controlled using a PID controller, which was applied to the first three joints. The effectiveness of the PID controller in tracking the desired path was evaluated using three different optimization techniques: Particle Swarm Optimization (PSO), Genetic Algorithm (GA), and Honey Badger Algorithm (HBA). These optimization algorithms were employed to fine-tune the PID parameters, enhancing the controller's performance in minimizing errors and improving the accuracy of the arm's movements. Fig. 7(b) depicts the relationship between the desired path and the actual path followed by the robotic arm under the control of the PID controller, optimized by the three techniques above. The results demonstrate the effectiveness of each optimization method in achieving precise path tracking. PSO, GA, and HBA each offer distinct advantages in optimizing the PID controller parameters, contributing to reduced error margins and enhanced control accuracy.

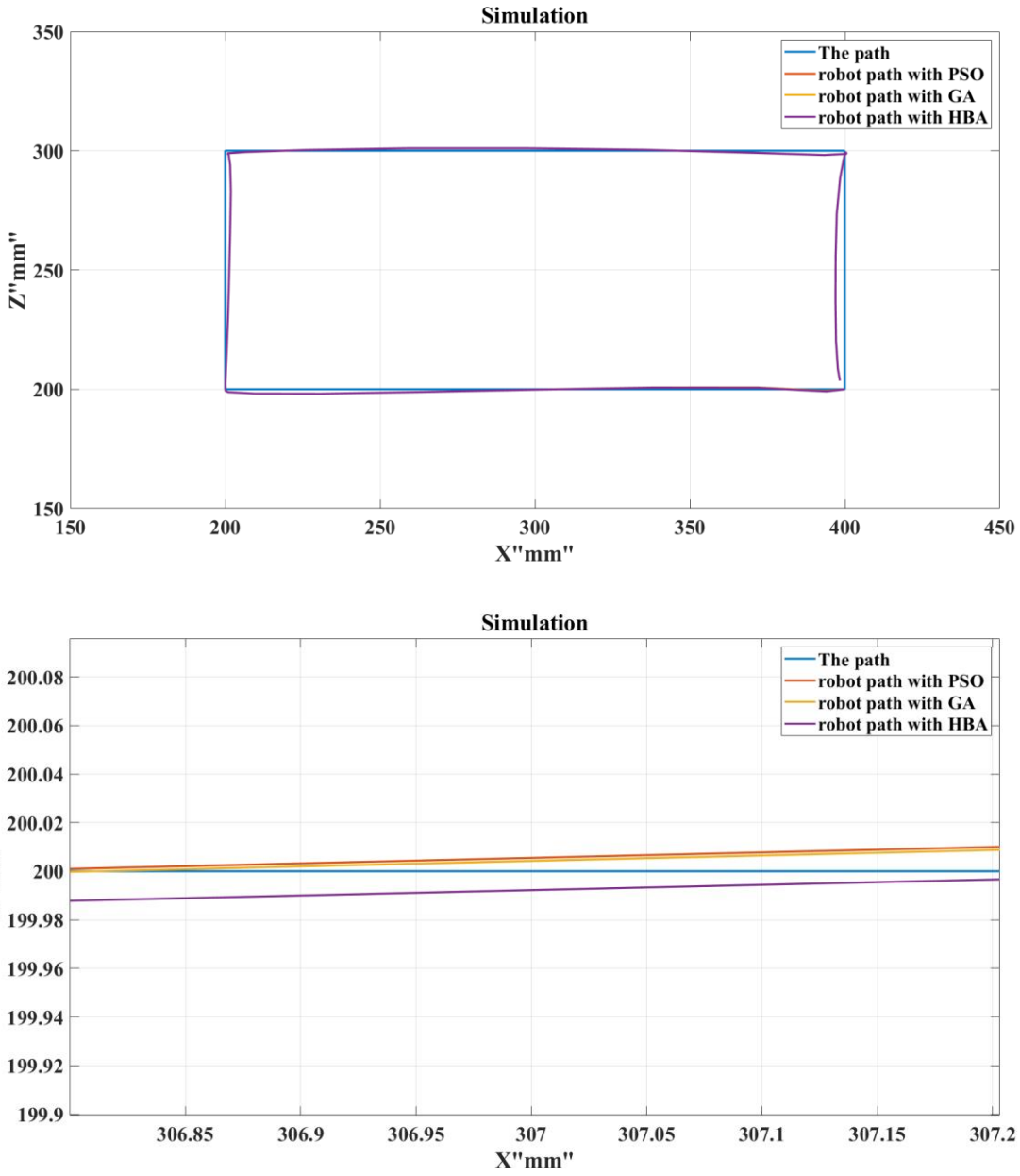

Fig. 8 (a) the desired path and the actual path with PID controller on the first 3 joints with PSO and GA and HBA. (b) more detailed view to notice the difference between the four paths.

7. Conclusions

This manuscript presents the development and optimization of a cost-effective, lightweight humanoid robotic arm designed to assist the elderly and vulnerable populations. By leveraging 3D printing technology, the arm achieves significant weight reduction while maintaining structural integrity and functionality. The incorporation of low-torque servomotors and an adaptable hand mechanism further enhances cost efficiency and operational capability. The study integrates human biomechanics into the design, ensuring that the robotic arm mimics the natural movements of a human arm. Forward kinematics, modeled using the Denavit-Hartenberg convention, provides precise calculations of the end-effector's position and orientation. The arm's six degrees of freedom enable a range of complex motions, critical for effective robotic assistance and rehabilitation. System identification through MATLAB has demonstrated high accuracy in joint movements, with fit percentages between 87.5% and 97.07%. The use of advanced optimization techniques such as Genetic Algorithm (GA), Particle Swarm Optimization (PSO), and Honey Badger Algorithm (HBA) to fine-tune the PID controller parameters has resulted in improved system responsiveness and precision. Experimental validation of the kinematic equations and control algorithms confirms the robotic arm's ability to follow a predefined three-dimensional path accurately. This validation underscores the system's reliability and potential for real-world applications.

References:

[1] Q. Huang *et al.*, "Historical Developments of BHR Humanoid Robots," *Advances in Historical Studies*, vol. 08, no. 01, pp. 79–90, 2019, doi: 10.4236/ahs.2019.81005.

[2] S. P. S. Yadav *et al.*, "Development of 3D Printed Electromyography Controlled Bionic Arm," in *Lecture Notes in Mechanical Engineering*, Springer Science and Business Media Deutschland GmbH, 2022, pp. 11–21. doi: 10.1007/978-981-16-2278-6_2.

[3] R. Siemasz, K. Tomczuk, and Z. Malecha, "3D printed robotic arm with elements of artificial intelligence," in *Procedia Computer Science*, Elsevier B.V., 2020, pp. 3741–3750. doi: 10.1016/j.procs.2020.09.013.

[4] A. C. Gheorghe, "Robotic Humanoid Arm," *The Scientific Bulletin of Electrical Engineering Faculty*, vol. 20, no. 1, pp. 37–39, Apr. 2020, doi: 10.2478/sbeef-2020-0108.

[5] L. PARALI, A. SARI, and M. ESEN, "Design of a 3D Printed Open Source Humanoid Robot," *Bitlis Eren Üniversitesi Fen Bilimleri Dergisi*, vol. 11, no. 2, pp. 411–420, Jun. 2022, doi: 10.17798/bitlisfen.998006.

[6] Mick, Lapeyre, Rouanet, Halgand, Benois-Pineau, Paclet,Cattaert, Oudeyer and de Rugy., "Reachy, a 3D-Printed Human-Like Robotic Arm as a Testbed for Human-Robot Control Strategies," *Front Neurorobot*, vol. 13, Jul. 2019, doi: 10.3389/fnbot.2019.00065.

[7] Z. Ali *et al.*, "Design and development of a low-cost 5-DOF robotic arm for lightweight material handling and sorting applications: A case study for small manufacturing industries of Pakistan," p. 101315, Jul. 2023, doi: 10.1016/j.rineng.2023.101315.

[8] G. Mantri, "DESIGN AND OPTIMIZATION OF PID CONTROLLER USING GENETIC ALGORITHM," *Int J Res Eng Technol*, vol. 02, pp. 926–930, Jul. 2013, doi: 10.15623/ijret.2013.0206002.

[9] D. Thangavelusamy and P. Lakshmi, "Comparison of PI controller tuning using GA and PSO for a Multivariable Experimental Four Tank System," *International Journal of Engineering and Technology*, vol. 5, pp. 4660–4671, Jul. 2013.

[10] S. Asif and P. Webb, "Kinematics Analysis of 6-DoF Articulated Robot with Spherical Wrist," *Math Probl Eng*, vol. 2021, 2021, doi: 10.1155/2021/6647035.

[11] M. Kim, S. Kim, S. Park, M.-T. Choi, M. Kim, and H. Gomaa, "Service robot for the elderly," *Robotics & Automation Magazine, IEEE*, vol. 16, pp. 34–45, Jul. 2009, doi: 10.1109/MRA.2008.931636.

[12] R. Riener, "Rehabilitation Robotics," *Foundations and Trends in Robotics*, vol. 3, pp. 1–137, Jul. 2012, doi: 10.1561/2300000028.

[13] J. Andrés-Esperanza, J. L. Iserte-Vilar, I. Llop-Harillo, and A. Pérez-González, "Affordable 3D-printed tendon prosthetic hands: Expectations and benchmarking questioned," *Engineering Science and Technology, an International Journal*, vol. 31, Jul. 2022, doi: 10.1016/j.jestch.2021.08.010.

[14] E. C. Agbaraji, H. C. Inyiama, and I. Obiora-dimson, "Joint Torque and Motion Computational Analysis for Robotic Manipulator Arm Design Department of Computer Engineering , Federal Polytechnic Nekede , Owerri , Nigeria Corresponding Author ' s E -mail : wattchux@gmail.com," vol. 12, no. June, pp. 1–9, 2018.

[15] J. K. Paik, B. H. Shin, Y. bong Bang, and Y. B. Shim, "Development of an Anthropomorphic Robotic Arm and Hand for Interactive Humanoids," *J Bionic Eng*, vol. 9, no. 2, pp. 133–142, Jun. 2012, doi: 10.1016/S1672-6529(11)60107-8.

[16] Y. Wang, W. Li, S. Togo, H. Yokoi, and Y. Jiang, "Survey on Main Drive Methods Used in Humanoid Robotic Upper Limbs," Jan. 01, 2021, *American Association for the Advancement of Science*. doi: 10.34133/2021/9817487.

[17] A. Yang, Y. Chen, W. Naeem, M. Fei, and L. Chen, "Humanoid motion planning of robotic arm based on human arm action feature and reinforcement learning," *Mechatronics*, vol. 78, Oct. 2021, doi: 10.1016/j.mechatronics.2021.102630.

[18] D. H. Gates, L. S. Walters, J. Cowley, J. M. Wilken, and L. Resnik, "Range of motion requirements for upper-limb activities of daily living," *American Journal of Occupational Therapy*, vol. 70, no. 1, Jan. 2016, doi: 10.5014/ajot.2016.015487.

[19] M. Elsamanty, E. M. Faidallah, Y. H. Hossameldin, S. M. Abd Rabbo, S. A. Maged, H. Yang, K. Guo, "Workspace Analysis and Path Planning of a Novel Robot Configuration with a 9-DOF Serial-Parallel Hybrid Manipulator (SPHM)," *Applied Sciences (Switzerland)*, vol. 13, no. 4, Feb. 2023, doi: 10.3390/app13042088.

[20] M. Elsamanty, E. M. Faidallah, Y. H. Hossameldin, S. M. Abd Rabbo, and S. A. Maged, "Design, simulation, and kinematics of 9-DOF Serial-Parallel Hybrid Manipulator Robot," in *2021 3rd Novel Intelligent and Leading Emerging Sciences Conference (NILES)*, Oct. 2021, pp. 370–375. doi: 10.1109/NILES53778.2021.9600537.

[21] S. S. Zhuwawu, A. B. Zaki, M. El-Samanty, V. Parque, and H. El-Hussieny, "Non-invasive Feedback for Prosthetic Arms: A Conceptual Design of a Wearable Haptic Armband," in *2023 IEEE/ASME International Conference on Advanced Intelligent Mechatronics (AIM)*, Jun. 2023, pp. 828–833. doi: 10.1109/AIM46323.2023.10196234.

[22] "System Identification Toolbox™ Getting Started Guide," 1988. [Online]. Available: www.mathworks.com

[23] D. Meena and S. Chahar, "Speed control of DC servo motor using genetic algorithm," Jul. 2017, pp. 1–7. doi: 10.1109/ICOMICON.2017.8279122.

[24] D. A. Souza, J. G. Batista, L. L. N. dos Reis, and A. B. S. Júnior, "PID controller with novel PSO applied to a joint of a robotic manipulator," Aug. 01, 2021, *Springer Science and Business Media Deutschland GmbH*. doi: 10.1007/s40430-021-03092-4.

[25] F. A. Hashim, E. H. Houssein, K. Hussain, M. S. Mabrouk, and W. Al-Atabany, "Honey Badger Algorithm: New metaheuristic algorithm for solving optimization problems," *Math Comput Simul*, vol. 192, pp. 84–110, Feb. 2022, doi: 10.1016/j.matcom.2021.08.013.

[26] A. Yang, Y. Chen, W. Naeem, M. Fei, and L. Chen, "Humanoid motion planning of robotic arm based on human arm action feature and reinforcement learning," *Mechatronics*, vol. 78, Oct. 2021, doi: 10.1016/j.mechatronics.2021.102630.